

# Design of meso-structured titanium oxo based hybrid organic–inorganic networks

Galo J. de A. A. Soler-Illia,<sup>a</sup> Emmanuel Scolan,<sup>a</sup> Audrey Louis,<sup>a</sup> Pierre-Antoine Albouy<sup>b</sup> and Clément Sanchez<sup>\*a</sup>

<sup>a</sup> *Chimie de la Matière Condensée, UMR CNRS 7574, Université Pierre et Marie Curie 4, place Jussieu, 75252 Paris, France. E-mail: clems@ccr.jussieu.fr*

<sup>b</sup> *Laboratoire de Physique des Solides, Université Paris-Sud, 91405 Orsay Cedex, France*

**Received (in Montpellier, France) 27th July 2000, Accepted 13th September 2000**

**First published as an Advance Article on the web 7th November 2000**

Titanium oxo clusters or nanosized Ti–O particles with hydrophobic or hydrophilic character can be obtained by varying the sol–gel synthesis conditions. These species are potentially interesting nano-building blocks (NBB) in the design of textured materials. The reactivity of well-defined hydrophobic NBB towards different nucleophiles has been characterised and discussed, in order to understand the processes taking place in the formation of meso-organised hybrids. Subsequently, different synthesis conditions were used to generate textured titania-based hybrid phases, using PEO-based surfactants as templating agents. The tuning of the interactions between the template and the different kinds of nano-building blocks allow worm-like and hexagonal titania-based hybrid phases to be reproducibly obtained.

## Introduction

The combination at the nanosize level of inorganic and organic or even bioactive components in a single material makes accessible a new area of materials science that has extraordinary implications for developing novel multifunctional materials exhibiting a wide range of properties.<sup>1–3</sup> Among soft chemical processes, sol–gel chemistry<sup>4</sup> offers a versatile access to new chemically designed hybrid organic–inorganic materials.<sup>5–10</sup> A deeper understanding and control of the semi-local and long range order structures of these materials is an important issue, especially if tailored properties are being sought.

“Organised matter sol–gel chemistry” is indeed a quickly developing area that has been growing throughout the last decade.<sup>11</sup> In this field, hybrid organic–inorganic phases are very interesting, due to the versatility they demonstrate in the building of a whole continuous range of nanocomposites, from ordered dispersions of well defined inorganic building blocks to highly controlled nanosegregation of organic polymers within inorganic matrices. In the latter case, one of the most striking examples is the synthesis of mesostructured hybrid networks, precursors of mesoporous solids.<sup>12</sup> All these highly controlled textured phases derive from oxo metal-based hybrid precursors, and in principle their construction can be tailored by the adequate use of sol–gel methods.

Such control over the growth and morphology of these materials can be achieved by following two main strategies: (i) the assembly of well-defined inorganic nano-building blocks (NBB) by using organic linkers;<sup>13</sup> (ii) the use of organic templates which self-organise into complex structures, patterning inorganic architectures built from molecular or NBB precursors.<sup>12,14</sup> Both strategies can yield a large variety of more or less textured nanocomposites depending on the nature of the hybrid organic–inorganic interface and the stability of the NBB towards the nucleophilic species that are present in the reaction bath.

In the construction of the mesostructured hybrid network, the interactions between the surface of the inorganic precur-

sors (molecular or NBB) and the organic texturing agent are of paramount importance. Traditional mesostructure synthesis routes resort to class I hybrid<sup>8a</sup> intermediates, which are based on hydrogen bonding, van der Waals or electrostatic forces that associate organic and inorganic components through weak interactions (at least in terms of orbital overlap).<sup>12a</sup> Another approach more recently developed (LAT, ligand assisted templating)<sup>12b,15</sup> is based on the chemical bonding (covalent, ionic-covalent or Lewis acid–base; *i.e.* class II hybrids)<sup>8a</sup> between molecular precursors and the complexing head groups of the surfactants, which in turn can give to the whole their self-organising properties. Both types of hybrids (Class I and II)<sup>8a</sup> could be useful in the synthesis of hierarchically organised materials. Class I hybrids generally allow more versatility in the tuning of the geometric and charge balance constraints needed at the interface to build highly ordered assemblies. Class II hybrid intermediates may also lead to the formation of ordered architectures providing that the strong chemical bonding occurring between the organic and the inorganic components does not drastically decrease the hydrophilic–hydrophobic difference between the different moieties forming the amphiphilic templates.<sup>16</sup>

Sol–gel methods permit one to create nanometric and monodispersed inorganic “bricks”, with great variety in their nature, structure and functionality. These inorganic supramolecular entities can be thoroughly characterised, facilitating the characterisation of the final materials. The use of nano-building blocks as starting units to obtain hybrid organic–inorganic structures is an approach developed with various systems such as oligosilasesquioxanes and derivatives,<sup>17–25</sup> organically functionalised heteropolyoxotungstates,<sup>26–33</sup> transition metal oxo clusters capped with polymerisable ligands<sup>34–36</sup> or connected through organic spacers (telechelic molecules or polymers, functional dendrimers)<sup>37</sup> and finally organotin oxo clusters.<sup>14,38–41</sup>

Depending on the set of experimental conditions chosen, these NBB can keep or not their integrity. Therefore they can be used as true building blocks that can be connected through organic spacers or surface driven condensation reactions or as

a reservoir of inorganic matter, which can be delivered at the hybrid interface to build an extended inorganic network.

A simple example which illustrates cluster stability towards nucleophilic reagents is provided by the chemistry of the cluster  $[(\text{BuSn})_{12}(\mu_3\text{-O})_{14}(\mu\text{-OH})_6]^{2+}2\text{OH}^-$  in which half of the tin atoms are fivefold-coordinated.<sup>38</sup> The positive charge of this dication is counter balanced by two  $\text{OH}^-$  anions that can be exchanged by sulfonate groups without affecting the integrity of the organotin oxo core.<sup>39</sup>

Such stability is strongly modified when the exchange process is made in the presence of carboxylic ligands. For a carboxy : cluster ratio  $>2:1$ , these clusters are cleaved yielding tin oxo carboxylate clusters  $\{\text{BuSnO}(\text{O}_2\text{CR}')\}_6$  ( $\text{R}'$  being any organic function), where the six tin atoms are sixfold-coordinated and complexed by bridging carboxylate ligands. However, for a carboxy : cluster ratio  $<2:1$ , hydroxide counter anions are exchanged by carboxylate groups without affecting the integrity of the tin oxo core. Under such conditions, these  $[(\text{BuSn})_{12}(\mu_3\text{-O})_{14}(\mu\text{-OH})_6]^{2+}$  clusters can be assembled through charge compensating organic dianions that bridge the clusters. This was achieved by treating  $[(\text{BuSn})_{12}\text{O}_{14}(\text{OH})_6][\text{OH}]_2$  with carboxymethyl terminated poly(ethylene glycol) (PEG) macromonomers or with organic diacids.<sup>40,41</sup>

Numerous titanium oxo clusters have been reported, with metal nuclearity ranging from 3 to 18.<sup>42–49</sup> They are potentially very interesting NBB precursors of titanium oxide-based hybrids and mesostructured titania. However, because of their size and the presence of reactive alkoxy groups on their surface, the titanium oxo core forming these nanobuilding blocks may exhibit poor stability in the presence of nucleophiles.

The research work reported in this article is presented in two parts: (i) First, a study concerning the stability of three highly condensed titanium oxo clusters ( $\text{Ti}_{12}\text{O}_{16}(\text{OPr}^i)_{16}$ ,  $\text{Ti}_{16}\text{O}_{16}(\text{OEt})_{32}$  and  $\text{Ti}_{18}\text{O}_{22}(\text{OBu}^n)_{26}(\text{acac})_2$ )<sup>42,43,46,49</sup> towards nucleophilic reagents is reported. The stability of the titanium oxo cores has been monitored by  $^{17}\text{O}$  NMR while the modifications undergone by the surface alkoxy groups have been probed through  $^{13}\text{C}$  NMR. (ii) Secondly, titanium oxo moieties ( $\text{Ti}_{16}\text{O}_{16}(\text{OEt})_{32}$ ) or inorganic NBB generated *in situ* by controlling the water amount and acidity are combined with organic non-ionic poly(ethylene oxide) (PEO)-based templates to obtain hybrid textured phases, which are precursors of mesoporous oxides. The resulting textured hybrid materials are characterised mainly by using XRD and TEM. Finally, a discussion on the role of the nature of the titanium oxo-based NBB and the effects of the amounts of water and acid used during the synthesis on the triggering of a given mesostructured phase is presented.

## Results and discussion

### (a) Stability and reactivity of Ti-based NBB

The use of pre-condensed species presents many advantages compared to alkoxide precursors: first, they exhibit a lower reactivity towards hydrolysis or attack of nucleophilic moieties; they are also monodisperse in size and chemical composition. Moreover, full characterisation performed by XRD, FTIR and multinuclear NMR allows one to separately analyse the modifications of the metal oxo core or the surface. Thus, they can be used as model systems to understand the construction of hybrid materials, particularly at the inorganic–organic interface.

Titanium oxo clusters can easily be obtained in a reproducible way by hydrolysis of  $\text{Ti}(\text{OR})_4$  in low water conditions (water to Ti ratio,  $h < 2$ , see Experimental for details). Fig. 1 presents the structure of the three studied clusters:

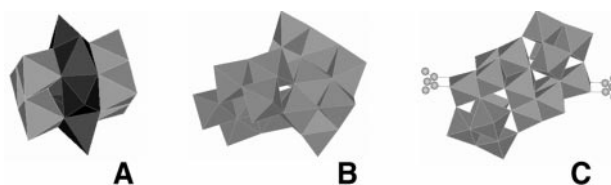


**Fig. 1** Molecular structures of (A)  $\text{Ti}_{12}\text{O}_{16}(\text{OPr}^i)_{16}$ , five-fold-coordinated sites are shown in black; (B)  $\text{Ti}_{16}\text{O}_{16}(\text{OEt})_{32}$  and (C)  $\text{Ti}_{18}\text{O}_{22}(\text{OBu}^n)_{26}(\text{acac})_2$ . Only the Ti–O cores are shown.

$\text{Ti}_{16}\text{O}_{16}(\text{OEt})_{32}$  (Ti16),  $\text{Ti}_{12}\text{O}_{16}(\text{OPr}^i)_{16}$  (Ti12) and  $\text{Ti}_{18}\text{O}_{22}(\text{OBu}^n)_{26}(\text{acac})_2$  (Ti18). They exhibit different structural features: the mean oxide core diameters are 9, 12 and 15 Å respectively. Half of the Ti atoms of the Ti12 oxo core are fivefold-coordinated while the remainder are sixfold-coordinated. The Ti16 and Ti18 cages contain only  $\text{TiO}_6$  octahedra. Finally, the nature (linear or ramified) and the bonding mode (terminal or bridging, mono- or bidentate) of the surface ligands are intrinsically different between these three titanium oxo clusters. All these structural differences can imply different reactivities in the presence of nucleophilic agents.

Solution NMR spectroscopy appears to be an efficient tool for probing the molecular environments of these clusters; therefore,  $^{17}\text{O}$  and  $^{13}\text{C}$  solution NMR have been performed to assess the stability of the oxometal core and the lability of the organic surface ligands respectively. The synthesis of the clusters in the presence of 10%  $^{17}\text{O}$  enriched water permits one to enhance the sensitivity of the technique by enriching the oxo bonds. The  $^{13}\text{C}$  and  $^{17}\text{O}$  chemical shifts of the different bridging oxygen atoms ( $\mu_i$ ,  $2 \leq i \leq 5$ ) of each cluster are summarised in the Experimental.

The reactivity of titanium oxo clusters with some low molecular weight alcohols has been reported.<sup>43,50,51</sup> The oxo core of  $\text{Ti}_{11}\text{O}_{13}(\text{OPr}^i)_{18}$ , Ti12 and Ti16 is stable towards ethanol or propanol. However, some of the alkoxide groups are exchanged by transalcoholysis reactions, giving rise to new species like  $\text{Ti}_{16}\text{O}_{16}(\text{OEt})_{24}(\text{OPr}^n)_8$  or  $\text{Ti}_{12}\text{O}_{16}(\text{OPr}^i)_{10}(\text{OEt})_6$ . On the other hand, clusters with lower nuclearity, such as  $\text{Ti}_7\text{O}_4(\text{OEt})_{20}$ , are destroyed by alcohol nucleophilic attack.<sup>50</sup> In view of the stability of Ti16 towards alcohols, diols can be used to establish connections between clusters. Fig. 2 presents the NMR spectra of a Ti16/1,3-propanediol system. The characteristic  $^{17}\text{O}$  and  $^{13}\text{C}$  resonances are broadened without loss of intensity for increasing diol quantities. This fact can be explained by a loss of mobility of the clusters in solution: an increase of the molecular size of the NMR probed species can lead to a subsequent broadening of the NMR resonances.  $^{13}\text{C}$  NMR spectra show the formation of ethanol ( $\delta_{\text{CH}_3}$  58) upon reaction. In all systems the quantity of free observable propanediol is very low; this confirms that ethoxide groups have been exchanged by propanediolate ligands, which bind to Ti16 by one or both extremities. The system can thus be described as aggregates of Ti16 clusters connected by diolate bridges. Similar behaviour has been reported previously in the reaction of  $\text{Ti}_{11}\text{O}_{13}(\text{OPr}^i)_{18}$  with diol compounds.<sup>51</sup> The authors have observed the formation of 100 to 1000 Å diameter particles (probed by quasi-elastic light scattering) and conclude that these particles are made up of interconnected clusters; diolate bridges interconnect the whole particle network. From our studies, we come to the same conclusions in the case of Ti16 with 1,3-propanediol.

In the case of a stronger nucleophile like acetylacetone (Hacac), the Ti–O core of Ti16 remains stable up to an  $n$  ratio ( $n = [\text{nucleophile}]/[\text{cluster}]$ ) of 4 (*cf.* Fig. 3), even after 15 days aging.  $^{13}\text{C}$  NMR spectra show that all the acetylacetone molecules are attached to Ti16 ( $\delta_{\text{CH}}$  103 for the bonded form (acac) and  $\delta_{\text{CH}}$  100 for the free form (Hacac) in solution). For

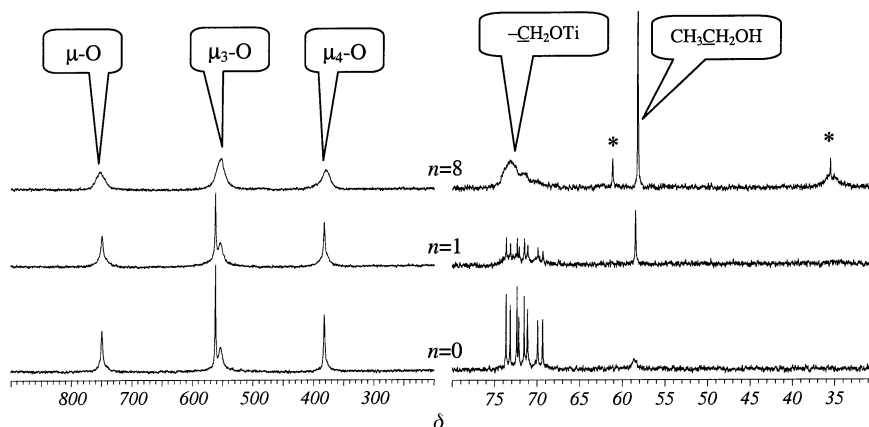


**Fig. 2**  $^{17}\text{O}$  (40.7 MHz; 5000 scans, left) and  $^{13}\text{C}$  (75.5 MHz; 2500 scans, right) NMR spectra of  $\text{Ti}_{16}\text{O}_{16}(\text{OEt})_{32}$  diluted with 1,3-propanediol (1,3 PD) at different  $n = [\text{1,3 PD}]/[\text{Ti16}]$  ratios; solvent  $\text{C}_6\text{D}_6$ -toluene (1 : 1). The  $^{13}\text{C}$  peaks marked with an asterisk correspond to excess of 1,3 PD.

higher  $n$  ratios the characteristic resonances of Ti16 oxo-bridges are less intense, and they are replaced by broad peaks that attest to the formation of larger species. Free Hacac in excess and ethanol are detectable and a new sharp resonance in the ethoxy region ( $\delta$  73) grows, which is characteristic of  $\text{Ti}(\text{OEt})_2(\text{acac})_2$  moieties resulting from cleavage of the Ti16 clusters.

Ti12 clusters are not stable in the presence of Hacac molecules and a ratio  $n = 4$  is enough to destroy all the cluster cores within 2 weeks of aging. For  $n = 12$  (Fig. 4), the characteristic cluster signals are replaced by broad and less intense resonances at  $\delta$  800 ( $\mu\text{-O}$ ), 550 ( $\mu_3\text{-O}$ ) and 350 (attributable to a mixture of  $\mu_4\text{-O}$  and bonded acac). The complexation of Ti by acac is confirmed by the appearance of free  $^i\text{PrOH}$  ( $\delta$  64) and linked acac ( $\delta_{\text{C=O}}$  188 and 192;  $\delta_{\text{C-H}_{\text{vinyl}}}$  103) in the  $^{13}\text{C}$  NMR solution spectra (not shown).

On the contrary, 100% (for  $n$  up to 8) and 80% (for  $n = 32$ ) of the Ti18 species remain untouched in the presence of Hacac

molecules, as determined by integration of the NMR peaks (Fig. 4B). For  $n < 8$ , free Hacac molecules in solution are in exchange with the chelating acac ligands on the cluster surface. In terms of stability towards Hacac and related nucleophiles such as acetoacetyethyl methacrylate (AAEM) and dibenzoylmethane (DBM), the observed differences between Ti12, Ti16 and Ti18 are mainly due to three causes. First, the presence of titanium atoms with unsatisfied coordination. While all Ti are octahedrally coordinated in Ti16 and Ti18, a corona of six out of twelve  $\text{Ti}^{\text{IV}}$  are five-coordinate in Ti12. This oxo core is more labile towards nucleophilic substitution. The stability of the Ti-O core also depends on the number of "bulk" oxo bridges, *i.e.* those with maximum coordination ( $\mu_4\text{-}$  and  $\mu_5\text{-O}$ ). Following this approach, Ti16 and Ti18 oxo cores are more compact when compared to Ti12; this stability seems not to depend on the Ti : O ratio. Finally, the presence of strongly chelated ligands at the surface of the clusters may impart an extra kinetic stability.

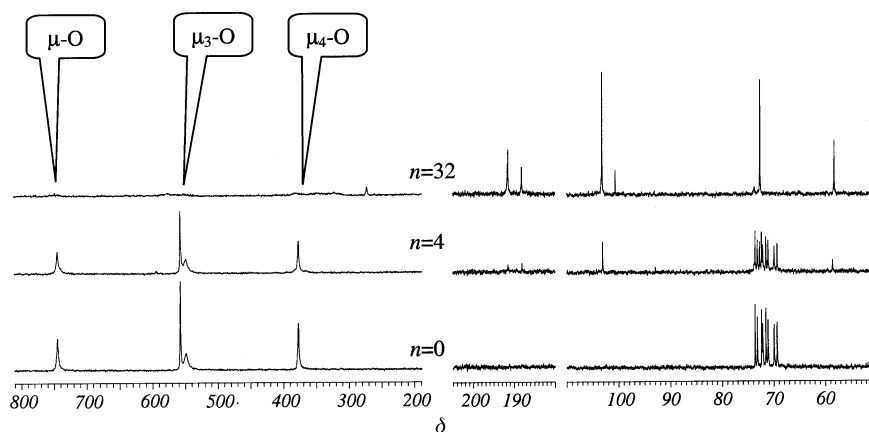


**Fig. 3**  $^{17}\text{O}$  (40.7 MHz; 5000 scans, left) and  $^{13}\text{C}$  (75.5 MHz; 2500 scans, right) NMR spectra (in  $\text{C}_6\text{D}_6$ -toluene, 1 : 1) of  $\text{Ti}_{16}\text{O}_{16}(\text{OEt})_{32}$  diluted with Hacac at different  $n$  ratios.

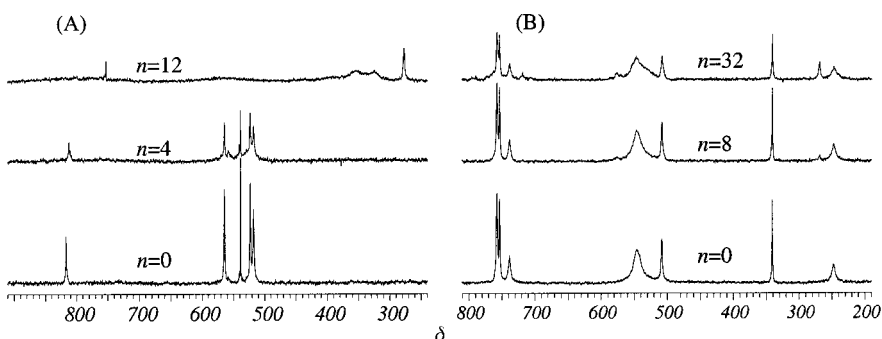


**Fig. 4**  $^{17}\text{O}$  (40.7 MHz; 5000 scans) NMR spectra of (A)  $\text{Ti}_{12}\text{O}_{16}(\text{OPr})_{16}$  and (B)  $\text{Ti}_{18}\text{O}_{22}(\text{OBu})_{26}(\text{acac})_2$  diluted with Hacac (in  $\text{C}_6\text{D}_6$ -toluene, 1 : 1) at different  $n$  ratios.

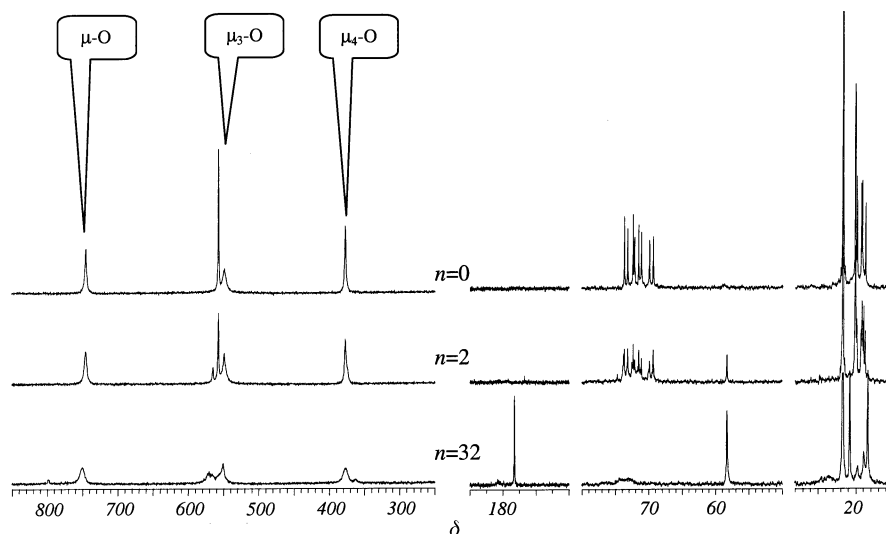


**Fig. 5**  $^{17}\text{O}$  (40.7 MHz; 5000 scans, left) and  $^{13}\text{C}$  (75.5 MHz; 2500 scans, right) NMR spectra (solvent  $\text{C}_6\text{D}_6$ -toluene, 1 : 1) of  $\text{Ti}_{16}\text{O}_{16}(\text{OEt})_{32}$  diluted with acetic acid at different  $n$  ratios.

Acetic acid (AcOH) is a frequently used bidentate ligand, and the study of its interaction with Ti16 allows us to evaluate the reactivity of NBB with carboxylic acid compounds. The behaviour of Ti16 in the presence of AcOH has been studied by NMR and FTIR. For  $n$  values up to 8 the integrity of the Ti-O core is preserved. However, some resonances are shifted in the  $^{17}\text{O}$  NMR spectra (from  $\delta$  557 to 565 and from 383 to 380) due to chelation of acetate groups on the clusters, see Fig. 5. This bonding on the surface is confirmed by  $^{13}\text{C}$  NMR spectra that show an increasing ethanol peak ( $\delta_{\text{CH}_2}$ , 58) with rising  $n$  values and a broadening and shifting of resonances in the ethoxy region ( $\delta$  69–74). Soluble acetic acid presents two forms in exchange: free in solution and chelated. FTIR spectra of  $n < 4$  systems (not shown) display the usual C-O bands of the alkoxy groups attached to the clusters (1143, 1097, 1072 and 1051  $\text{cm}^{-1}$ ) and additional bridging acetate bands at 1535 and 1441  $\text{cm}^{-1}$ .<sup>52</sup> For higher  $n$  values, solutions become turbid and gel, due to water produced from esterification reactions between free acetic acid and formed ethanol. In this case FTIR spectra clearly display OH bands (3500  $\text{cm}^{-1}$ ), excess acetic acid (weak band at 1700  $\text{cm}^{-1}$ ), ethyl acetate (1740  $\text{cm}^{-1}$ ) and a wide absorption at low frequencies (400–900  $\text{cm}^{-1}$ ) due to the formation of an extended titanium oxo network.

The stability of the Ti16 oxo core with a water to Ti ratio of 2 : 1 was probed using solid state  $^{17}\text{O}$  MAS NMR on a white precipitate obtained after hydrolysis of  $^{17}\text{O}$  enriched Ti16 with  $^{17}\text{O}$  enriched or unenriched water. The spectra (see Fig. 6) display the same resonances that those observed for Ti16 crystals, except that the peaks are slightly broader.<sup>53</sup> Two new resonances at  $\delta$  700 and 510 can be attributed to  $\mu\text{-}$  and  $\mu_3\text{-O}$  inter-cluster bridges respectively.<sup>53</sup> The resonances at  $\delta$  170 and  $-35$  can be assigned to Ti-OH<sup>54</sup> groups and adsorbed water<sup>55</sup> respectively. The conservation of the Ti16 core is in agreement with previously published results.<sup>50</sup> It has also been suggested that Ti12 clusters do not react with water, provided that the reaction is conducted in the parent alcohol and in the presence of low quantities of water (*i.e.* a 0.3 mol  $\text{dm}^{-3}$  cluster solution in  $^i\text{PrOH}$ , 4 equivalents of water per cluster,  $n = 0.33$ ). On the contrary, in non-polar media (toluene-acetonitrile mixtures) white precipitates are readily obtained.<sup>43</sup>

In conclusion, the studied titanium oxo clusters exhibit different reactivity to a wide variety of nucleophilic species, that can be summarised as follows: the acidity of the entering species plays an important role in the kinetics of substitution; mild nucleophiles, such as alcohol (or diol) compounds, leave the cluster core untouched, water can hydrolyse surface

groups, thus leading to connection; nucleophiles bearing chelating functions (carboxy, acetoacetyl, *etc.*) can modify the core, by chelation of the metal centres. (This can destroy the clusters. The effectiveness of the cleavage follows the sequence  $\text{Ti18} < \text{Ti16} \ll \text{Ti12}$ .)

The presented data on the reactivity of titanium oxo clusters can be advantageously applied to the design of new materials with tailored textures. As an example, dendrimers<sup>56</sup> have been used as polyfunctional connectors of Ti16 nano-building blocks. The nucleophilic reactions between  $-\text{Ph}-\text{CH}_2\text{OH}$  and  $-\text{CO}_2\text{H}$  functionalised dendrimers and the titanium(IV) centres of the Ti16 clusters form the hybrid interface. The covalent bonding between the dendrimers and the clusters was evidenced through  $^{13}\text{C}$  MAS NMR and FTIR:<sup>37</sup> the reaction implies the substitution of two coordination positions of vicinal Ti atoms. This reaction is limited to the surface of the cluster; the integrity of the titanium oxo core in the final hybrid solid was checked through solid state  $^{17}\text{O}$  NMR measurements. The obtained bicontinuous xerogels are in fact locally ordered dispersions of Ti16 clusters with correlation distances of about 2 nm and coherent scattering domains (CSD) of 5–6 nm. The symmetry of the organic template, as well as the capability for cluster anchoring, are essential features in the synthesis of meso-organised hybrid dispersions. Another important point is the control of reactions at the

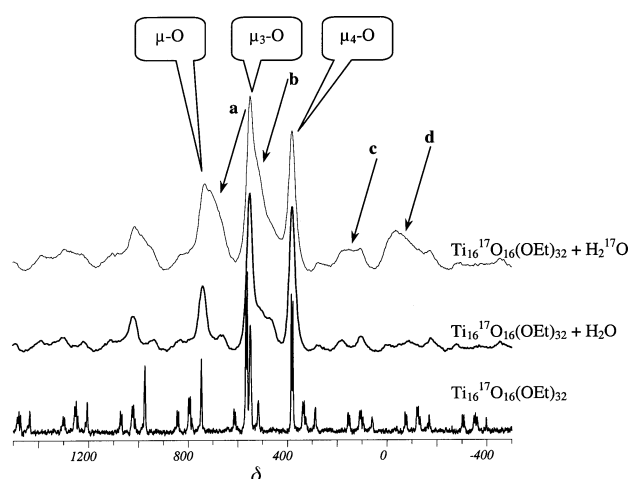


**Fig. 6**  $^{17}\text{O}$  MAS NMR spectra recorded at 54.25 MHz for  $\text{Ti}_{16}\text{O}_{16}(\text{OEt})_{32} + 32 \text{ H}_2\text{O}$  at 15 kHz spinning rate (8192 scans). Arrows indicate the new resonances not belonging to Ti16 clusters: (a)  $\mu\text{-O}$  intercluster; (b)  $\mu_3\text{-O}$  intercluster; (c) surface TiOH groups; (d) hydration water. See references in the text.

interface level between the organic template and the inorganic building unit, in order to preserve the  $\text{Ti}_{16}\text{O}_{16}$  oxo core.<sup>37</sup>

The  $\text{Ti}_{16}$  clusters can also be considered as an interesting brick for more complex systems, for example in the construction of precursors for mesoporous titania. These results will be discussed in the next section.

#### (b) Self assembly in texturing systems: role of the template–metal interactions

One of the major problems in texturing transition metals is the high reactivity of metal alkoxide precursors towards hydrolysis-condensation reactions, which usually leads to a very fast nucleation, promoting an uncontrolled segregation of a dense oxidic phase. In principle, there are two ways to control the fast processes of hydrolysis and condensation, and these have been thoroughly studied in the case of Ti. The first approach consists of working in diluted alcoholic media with  $\text{Ti}_{16}$  NBB or with very low water to metal ratios ( $h = \text{H}_2\text{O}/\text{Ti} < 2$ ). In this way, sets of hydrophobic low-nuclearity Ti–O alkoxo entities are obtained, which are similar to the clusters of the previous section, but polydisperse in size and chemical composition. The second approach consists of the addition of condensation inhibitors such as chelating agents (acetylacetone,<sup>57</sup> alcohol amines,<sup>58</sup> peroxide<sup>59</sup>) or mineral acids (in which  $p = [\text{HX}]/[\text{Ti}]$ ). Anhydrous or acid-inhibited systems have been prepared that differ in their  $h$ ,  $s$  ( $s = [\text{Ti}]/[\text{surfactant}]$ ) and  $p$  values, with various PEO-based surfactants as templating agents (see Experimental). The initial transparent sols gave rise to different kinds of solids, depend-

ing on their composition and treatment. Table 1 summarises the properties of representative samples.

**Media with low water content.** Homogeneous xerogels are obtained by slow evaporation of low water content solutions in Petri dishes; at the same time, moisture can provide a continuous and gentle input of water. Fig. 7 shows the XRD patterns obtained for titanium hybrid phases using different polymers as texturing agents (see also Table 1). In all cases, bicontinuous worm-like phases are obtained, as demonstrated by TEM images (Fig. 7). This kind of texture has been obtained previously in silica, alumina and  $\text{SiO}_2\text{--TiO}_2$  systems, in the presence of PEO-based surfactants.<sup>60</sup> The broad diffraction peaks coincide with the mean separation of the inorganic walls of the channels determined by TEM. These channels display characteristic sizes in the range 25–50 Å. These characteristic correlation distances do not change appreciably even when the mass of the templating agent is changed from 1000 D (P3100) to *ca.* 13 000 D (F127). There is, however, a small continuous change with surfactant contents, *i.e.* the mean distances are lower for higher inorganic contents. Surfactants act in these systems as flexible spacers of the inorganic network.

Although these phases do not display long range order, they can give rise to high surface area solids ( $S \approx 250 \text{ m}^2 \text{ g}^{-1}$ ) when thermally treated under appropriate conditions. The thick walls do not collapse, and the whole worm-like motif is conserved; similar behaviour has been reported for this kind of surfactant.<sup>60</sup> The XRD peaks become sharper upon

**Table 1** Properties of mesostructured Ti/polymer hybrids

Surfactant	Titanium precursor	Solvent	Final solid	Water content $h = \text{water}/\text{Ti}$ (mol/mol)	Acid content $p = \text{HCl}/\text{Ti}$ (mol/mol)	$s = \text{Ti}/$ surfactant (mol/mol)	Obtained texturation	$d_{100}/\text{\AA}$
F127	TBT	EtOH	Xerogel	0.06	0.015	135	Vermicular	19
	TET	EtOH	Precipitate	3.76	1	70	Hexagonal	114
	TBT	BuOH	Xerogel	25	1	70	Hexagonal	167
P123	TBT	EtOH	Xerogel	0.06	0.015	60	Vermicular	28
Brij 56	TPT	<sup>i</sup> PrOH	Precipitate	11.3	3	20	q-Hexagonal	45
	TET	EtOH	Xerogel				q-Hexagonal	55
			Xerogel				q-Hexagonal	46
P3100	TBT	BuOH	Xerogel	0.06	0.015	50	Vermicular	31
L35	TET	EtOH	Xerogel	3.76	1	50	q-Hexagonal	18
Syn 42	$\text{Ti}_{16}$	THF	Xerogel	<sup>a</sup>	<sup>a</sup>	8	Vermicular	47
P3100	cluster		Xerogel	<sup>a</sup>	<sup>a</sup>	8	Vermicular	35

<sup>a</sup> No water was added to these systems, except that arising from moisture or traces present in the surfactants or solvents.

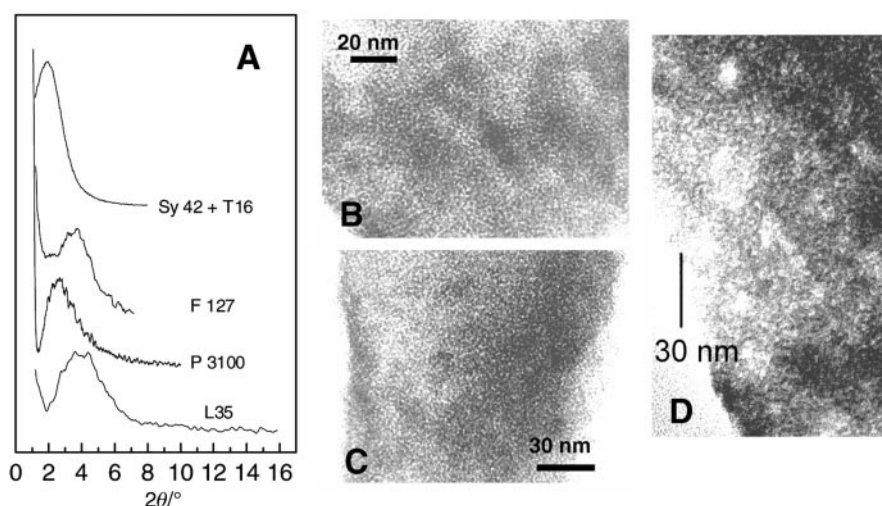


**Fig. 7** (A) XRD patterns of titanium oxide: block copolymer systems with different texturing agents.  $s$  values (from top to bottom) 32, 70, 50, 50. (B) TEM image of a worm-like TBT/P3100/BuOH sample,  $s = 50$ ,  $h = 0.06$ . (C) TEM of a TET/F127/EtOH hybrid;  $s = 130$ ,  $h = 0.06$ . (D) TEM image of the calcination product of a  $\text{Ti}_{16}$ /Syn 42 hybrid,  $s = 32$ .

thermal treatment, and the contrast under TEM is improved. Condensation is completed in the first stages, at *ca.* 200 °C, as shown by TG (an exothermic peak at 200 °C corresponds to the liberation of RO-blocked positions and subsequent condensation of the inorganic network) and FTIR (O–H stretching at 3500 cm<sup>-1</sup>,  $\delta_{\text{H}_2\text{O}}$  1650 cm<sup>-1</sup>).

The inadequate folding of the template in the stages previous to the formation of the hybrid is responsible for the lack of long-range order of these phases. In principle, there are three main interactions that control the folding of the polymers to yield a self-assembled hybrid liquid crystalline (LC) mesophase: polymer–polymer, inorganic–inorganic and polymer–inorganic; the contributions of these to the total free energy of the system have been stated in previous works.<sup>62</sup> The complex balance of these interactions can lead to a wide range of mesostructures. In the case of transition metals and PEO-based surfactants particular attention has to be paid to the interactions between the template and the inorganic components. These are strongly dependent on the solvent, undergoing important and continuous modifications with ageing of the reaction systems, as will be discussed below.

The difference in hydrophobicity/hydrophilicity between the PEO and poly(propylene oxide) (PPO) chains in low water content alcoholic media is not marked enough to give rise to LC phases in the initial systems.<sup>63</sup> Enhancing the solubility differences of the texturing agents {as in the case of PEO–PBO–PEO [PBO = poly(butylene oxide)]} should lead to a better ordering; this has been demonstrated in the case of systems made up silica/block copolymers.<sup>64</sup> The presence of water increases the segregation between both blocks. Moreover, it has been demonstrated (for silica/CTAB (cetyltrimethyl ammonium bromide systems)<sup>65</sup> that the presence of low molecular weight alcohols can affect organisation in a negative way. The scarce water present in low water content systems reacts promptly with the alkoxide, generating a set of hydrophobic clusters under these conditions.<sup>66</sup> These Ti–O clusters, similar to those described in the previous section, can attach loosely to the hydrophobic PPO block; this process also tends to destabilise the formation of a well-ordered mesophase.

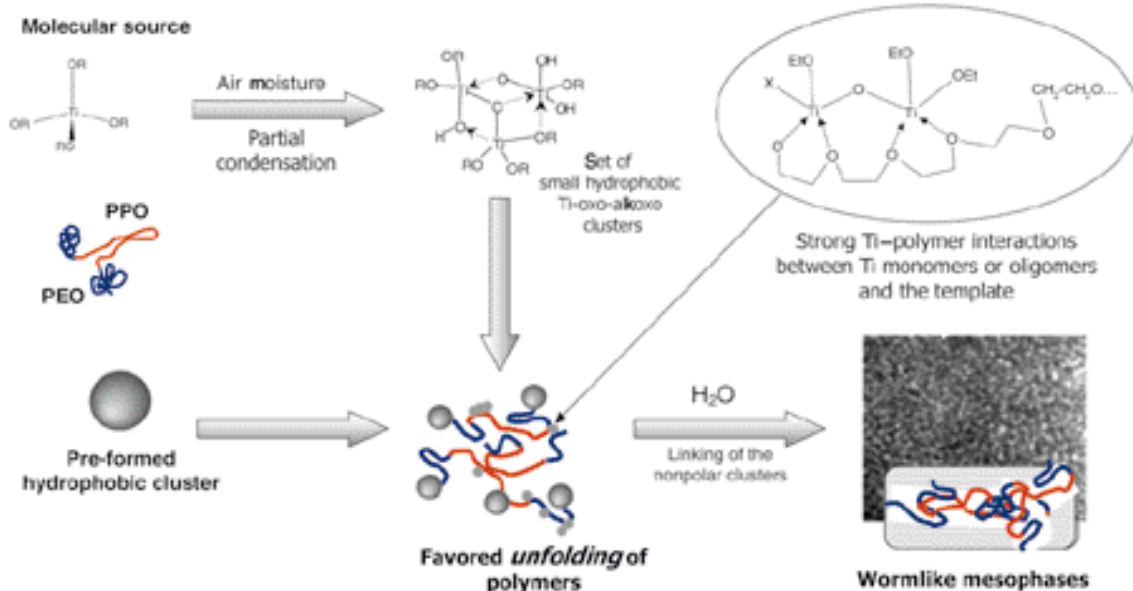
This has been tested by using Ti16 building blocks as pre-condensed inorganic precursors in the presence of moisture as the only water source. Under these conditions, as previously discussed, water molecules connect the clusters without cleaving the titanium oxo core. These reactions also lead to the

formation of bicontinuous worm-like gels (*d* spacing = 35–47 Å, see *e.g.* Table 1 and Fig. 7D).

The strong interactions between metal centres and the texturing agent are also an important issue. There are two essential interactions that lead to unfolding of the polymer: transalcoholysis of the –CH<sub>2</sub>–CH<sub>2</sub>–OH tips on the TiO<sub>h</sub>(OR)<sub>4-h/2</sub> moieties ( $0 < h < 2$ ), and chelation of titanium(IV) ions or oligomers by PEO or PPO blocks.<sup>16</sup> In the first case the hydrophobic species attached to the hydrophilic ends of the polymer alters the formation of a LC mesophase; this effect is even more marked in polymers with a small PEO block. When the  $\cdots\text{O}-\text{CH}(\text{R})-\text{CH}_2-\text{O}\cdots$  species coordinate to Ti<sup>IV</sup> the subsequent construction of the inorganic phase develops along the polymer skeleton, and not only at the solution–PEO interface. These strong interactions are hindered in the presence of polar solvents;<sup>16</sup> however, they are enhanced while drying. It should be recalled that under conditions where  $h < 2$ , drying and condensation are co-operative processes, that run in a parallel way. The unfolding process disrupts the formation of an organised LC phase, based upon the self-assembly properties of the polymer. As a consequence, ill-defined channels develop all along the sample, which ends up as a bicontinuous phase. In this scenario (set of hydrophobic clusters and strong Ti–polymer interactions) a further input of water can lead to cluster connection (Scheme 1). An excess of water, thus, is needed to attain a well ordered mesophase. The fine tuning of water is critical, as its function is twofold: formation of the inorganic skeleton, and promotion of an adequate template folding.

**Media with high water content.** Xerogels or precipitates can be obtained by hydrolysis-condensation of titanium alkoxide precursors in acidic media in the presence of texturing agents, see Experimental; texturation of the hybrid phases can greatly be improved by adding even low quantities of acidic water to the reacting systems. XRD patterns display more and sharper peaks (including a very strong diffraction at low-angle distances between 110 and 170 Å, for F127) depending on the initial conditions, as shown in Fig. 8. The better ordering suggested by XRD is confirmed by TEM images; the retrieved distances correspond mainly to the [100] reflections of a 2-D hexagonal or slightly distorted hexagonal mesophase (q-hex).

The F127/TBT system depicted in Fig. 8 provides an example of a titania-based mesostructured hybrid obtained by



**Scheme 1** Formation of hybrid wormlike phases in low water content systems. The strong (covalent) interactions between the texturing agent and the metal centres hinder the proper folding of the PEO-based surfactants; the resulting formation of the inorganic network occurs along the deployed polymers.



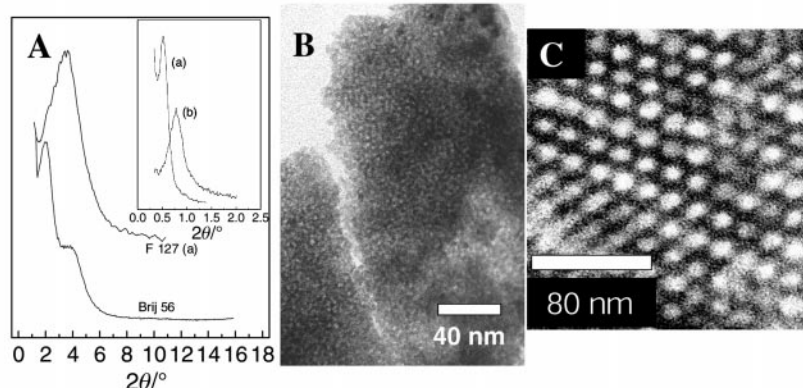


**Fig. 8** (A) XRD patterns of hybrid precursors obtained from titanium alkoxides under acidic conditions. Inset: low angle XRD of TBT/F127/BuOH/HCl hybrid ( $s = 70$ ,  $h = 25$ ,  $p = 1$ ) (a) and TET/F127/EtOH/HCl hybrid ( $s = 70$ ,  $h = 3.76$ ,  $p = 1$ ) (b). (B) TEM image of mesostructured titania obtained by thermal treatment of a TPT/Brij 56/ $i$ PrOH hybrid,  $s = 20$ ,  $h = 11$ ,  $p = 3$  (XRD shown in A). (C) TEM of the hybrid TBT/F127/BuOH/HCl;  $s = 70$ ,  $h = 25$ ,  $p = 1$  (XRD shown in A and inset a).

precipitation. The distance between the organic pores is *ca.* 190–200 Å, while  $d_{100} = 167$  Å ( $d_{100\text{TEM}} \approx 170$  Å). These values are slightly larger than those reported by Yang *et al.*, who found typical  $d_{100}$  values of 123 Å with a lower molecular weight polymer such as P123 for a mesostructured titania-based hybrid.<sup>67</sup> Comparable sizes are found in F127-templated cubic silica (SBA-16,  $a = 176$  Å)<sup>68</sup> and 3-D-hexagonal-textured silica fibres ( $a = 158$ ;  $c = 253$  Å).<sup>69</sup> The reported synthesis of textured silica and titania has been performed mainly in ethanol–water systems, yielding mostly cubic silica phases when using F127 as the template. The great proportion of EO groups in F127 favours the formation of high curvature phases (micellar, cubic, *etc.*), as has been demonstrated in pure aqueous solutions.<sup>70</sup> However, butanol can act like a co-surfactant causing a decrease in the curvature, and enhancing the hexagonal domain. The composition of our initial systems corresponds approximately (the changes due to the presence of HCl and titanium alkoxide species are not taken into account) to the domain of a 2-D-hexagonal lyotropic mesophase (order parameter 130–150 Å).<sup>71</sup> It is likely that the formation of the inorganic network takes place within this textured environment. The thickness of the inorganic walls is *ca.* 75 Å, which agrees well with previous data on silica/F127;<sup>68</sup> the diameter of the pores is *ca.* 100 Å. The phases obtained from TET/F127/EtOH/acid systems display lower ordering distances (110 Å); this may be due to the fact that ethanol does not act as a swelling agent.

Brij 56 has also been used as a texturing agent, giving rise to mesostructured powders or xerogels. All samples display two well-defined diffraction peaks corresponding to the [100] and [200] lines of an ordered superstructure (Fig. 8A). TEM shows homogeneous quasi-hexagonal arrangements (Fig. 8B). These can be described as arrays of clearly defined pores that do not present a perfect hexagonal symmetry, albeit they do not show the typical worm-like channel pattern. The reported  $d$  values (see Table 1) are in good agreement with those obtained for similar systems in the cases of silica-based<sup>60</sup> molecular sieves (40–50 Å), and they are larger for TET/ethanol systems than for TPT/ $i$ PrOH mixtures (Table 1). These values also decrease when the inhibitor ratio,  $p$ , is increased, in the case of TET/EtOH. Both facts suggest that more reactive systems (either with a lower inhibition ratio, or with a more reactive starting alkoxide) lead to hybrids with lower ordering distances. This can also be the case with the previously presented F127 solids. Thermal treatment of these precursors gives rise to high surface textured anatase; these studies will be the subject of a further paper.<sup>61</sup>

In the synthesis of hybrid mesophases by the high water contents route (*i.e.*  $h \gg 2$ ) the role of water as a texturant is enhanced as much as possible. At the same time the presence

of highly reactive transition metal centres (hydrolysis and subsequent polycondensation processes are practically instantaneous under these conditions requires blocking of the role of water as a polymerisation agent. Addition of mineral acids is a widely known way to control the formation of nanosized phases in sol–gel chemistry.<sup>72</sup> In the presence of this kind of inhibitor, the condensation process ends up by forming discrete oxo oligomers, of general formula  $\text{TiX}_x(\text{OH})_y\text{O}_{2-(x+y)/2}$  ( $X = \text{OR}$  or even  $\text{Cl}$ ; for high  $h$  and  $p$ ,  $x \leq 0.2$ ,  $y \approx 0.2$ – $0.5$ ).<sup>66,73</sup> A recent study has shown that in acidic media and high water contents these species bear surface OH groups that make them hydrophilic; their gyration radius has been determined by small angle X-ray scattering (SAXS) to be in the order of 20 Å and approximately half of the titanium(IV) ions are located on the surface.<sup>53,66</sup> They are positively charged in our highly acidic media, as the pH values reached are well below the point of zero charge (p.z.c) ( $\approx 6.5$ ) for any  $\text{TiO}$  phase.<sup>74</sup> These entities are in fact the building blocks of highly branched fractal Ti–O polymers, which are built up from the co-condensation of these sub-units.<sup>66</sup>

The co-condensation rate depends on the concentration of these sub-units. Two situations can be envisaged, that can lead to the formation of mesostructures amorphous titania-based hybrids. If the concentration of the precursor sol is high enough, precipitates can be obtained; this process depends crucially on the interactions between the titania sub-units and the polymer. In highly acidic media, chelation of titanium(IV) centres by the PEO or PPO blocks or transalcoholysis of the remaining alkoxo groups by the –OH ends of the polymers are strongly unfavoured.<sup>16</sup> The hydrogen-bonding interactions between the hydrophilic sub-units and the polymers should be predominant. The high proton (and chloride) concentration may also allow for the development of some positive charge over the EO and PO groups; consequently, a chloride-mediated electrostatic interaction of the type  $[\text{polymer H}]^+ \cdots \text{Cl}^- \cdots [\text{sub-unit}]^+$  can be envisaged as well. Moreover, a similar effect has been reported in  $\text{TiCl}_4/\text{EtOH}/\text{P123}$  systems, where chloride anions were present in precursors of mesoporous  $\text{TiO}_2$ , probably forming part of the hybrid interface.<sup>67b,67b</sup> Once formed, this weak hybrid interface can have a role in the nucleation of structured precipitates. An ordered aggregation of the sub-units around well-defined micelles followed by co-condensation gives way to the mesostructured hybrid; it has been suggested that these processes are similar to precipitation of polyelectrolytes in the presence of surfactants.<sup>75</sup> This gives rise to a relatively compact packing of the sub-units, leading to formation of the inorganic network. However, the systems are far from complete condensation; trapped water, incompletely removed EtO groups and EtOH are present in all obtained solids. FTIR and

TGA gave similar results as in the previous section (see above).

If solutions are dilute enough, subsequent solvent (and HCl) evaporation opens the way for slow aggregation of the sub-units. The evaporation of the alcohol promotes improved segregation of the PEO and PPO blocks, and the presence of water improves folding of the polymer and hence the mesophase structuration (Scheme 2). The ultimate mesostructure of the final solid depends on the competition between the connection reactions of the titania sub-units and the elimination of the solvent, some of which can remain trapped, while an extended bicontinuous gel is forming.

The results presented in this section illustrate two different synthesis paths that lead to mesostructured hybrid titania. Two important features have been identified, aside of classical synthesis variables. The first concerns the nature of the interactions at the hybrid interface, that determine the folding of the texturing agent, and therefore the final structuring. As previously suggested,<sup>62</sup> these depend mainly on the relative strength of the polymer-to-metal coordination *vs.* the polymer–polymer (*i.e.* the hydrophilic–hydrophobic balance) or polymer–solvent interactions. Another key point is that the precursors arising from low or high water content conditions are radically different. Clusters synthesized under conditions where  $h < 2$ , being hydrophobic, promote unfolding of the polymers, leading to poor texturation. In contrast, in acidic aqueous systems, where condensation is adequately blocked, more hydrophilic sub-units are generated.<sup>76</sup> In the presence of pluronic templates, these are interesting building blocks for the formation of well-defined hybrid mesophases.

## Conclusion

It has been shown that the stability of the titanium oxo core towards nucleophilic species of three titanium oxo clusters of high nuclearity  $\text{Ti}_{12}\text{O}_{16}(\text{OPr}^i)_{16}$ ,  $\text{Ti}_{16}\text{O}_{16}(\text{OEt})_{32}$  and  $\text{Ti}_{18}\text{O}_{22}(\text{OBu}^n)_{26}(\text{acac})_2$  depends on several parameters such as the cluster nuclearity, the presence of titanium atoms with unsatisfied coordination (lower than 6), the presence of oxygen atoms located in the bulk of the cluster ( $\mu_4\text{-O}$  and  $\mu_5\text{-O}$  bridges) and the presence of bidentate ligands.

All three clusters are stable in the presence of alcohols or polyols and only undergo transalcoholysis reactions of their alkoxy groups. These simple reactions can thus be used for

cluster functionalisation. Therefore under these conditions they can be used as nanobuilding blocks to obtain hybrid organic–inorganic structures *via* organic polymerisation of polymerisable alkoxy groups<sup>13,36</sup> or through cross-linking reactions using organic spacers such as polyols or alcohol functionalised dendrimers.<sup>37</sup>

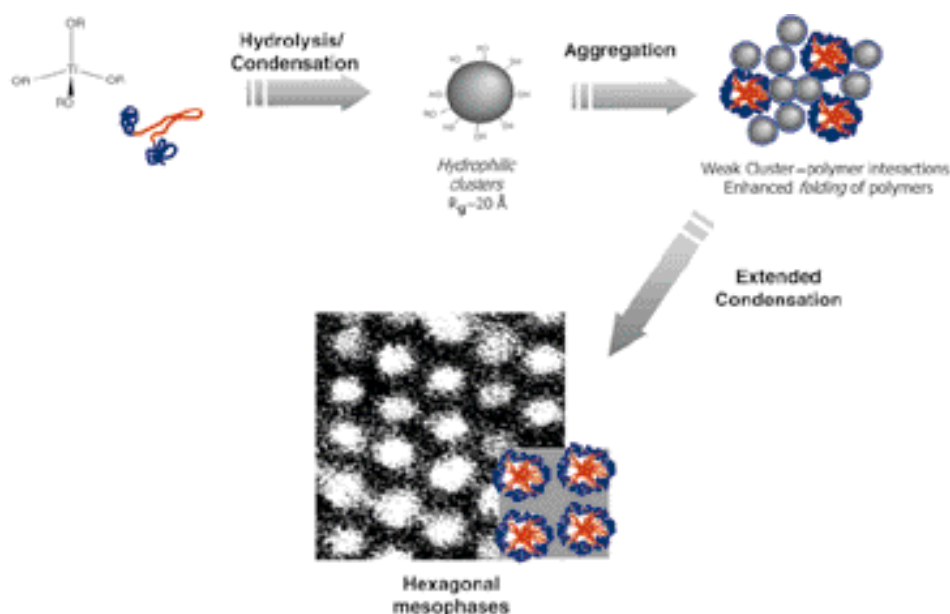
In the presence of controlled amounts of water the integrity of the titanium oxo cores can be conserved, depending on the solvent used. As previously reported,<sup>43,50</sup> a set of conditions can be determined where reactions can be circumscribed to their surface groups, which after hydrolysis lead to condensation reactions between the NBB. Their stability towards strong complexing ligands (carboxylate, acetylacetonate, *etc.*) can be classified as follows:  $\text{Ti}_{12}\text{O}_{16}(\text{OPr}^i)_{16} \ll \text{Ti}_{16}\text{O}_{16}(\text{OEt})_{32} < \text{Ti}_{18}\text{O}_{22}(\text{OBu}^n)_{26}(\text{acac})_2$ . The first cluster is easily cleaved even in the presence of small amounts of complexing bidentate ligands ( $\text{RCO}_2\text{H}$  or Hacac) while the two others keep their integrity until  $\text{RCO}_2\text{H} : \text{Ti}$  and Hacac : Ti ratios of 0.25 and 0.5 : 1 for  $\text{Ti}_{16}\text{O}_{16}(\text{OEt})_{32}$  and  $\text{Ti}_{18}\text{O}_{22}(\text{OBu}^n)_{26}(\text{acac})_2$  respectively.

The self assembly of nanobuilding blocks is an interesting approach to achieve control of the texture of transition metal oxo-based hybrid materials, due to the possibility of cluster connection. The combination between the “nanobuilding block approach” and templated assembling has been tested with pluronic templates. The interactions between PEO-based templates and transition metal oxo clusters are key in the synthesis of mesostructured materials.

In low water content media, strong chelation between hydrophobic clusters generated *in situ* or modelled through the use of  $\text{Ti}_{16}\text{O}_{16}(\text{OEt})_{32}$  and non-ionic polar heads leads to polymer unfolding, and thus to worm-like phases.

Larger quantities of water and acid added to the reaction bath play a double role: they blur the coordination bonds that comprise the hybrid interface yielding weak interactions (mainly hydrogen bonding) and allow the formation of nano-sized hydrophilic building blocks. These hydrophilic species may eventually interact during drying with the PEO polar heads therefore increasing the solubility difference between the amphiphilic block of the polymeric templates. Both contributions will improve folding of the templating agents, and yield more ordered mesophases.

The use of surfactant templates with amphiphilic components exhibiting a strong solubility difference even after



**Scheme 2** Formation of hybrid hexagonal phases in high water content systems. Hydrophilic species are formed, that can interact with the structuring polymers *via* hydrogen bonding. This results in a more pronounced differentiation of the amphiphilic blocs, leading to phase segregation on the nanometric scale; this permits the construction of more ordered phases.



coordination with the NBB will enhance segregation of the texturing agent, allowing for the design of highly ordered hybrid mesostructured phases.

## Experimental

### Starting materials

The inorganic precursors used for the synthesis of mesostructured titania were titanium alkoxides:  $\text{Ti}(\text{OEt})_4$  (TET) (purity ca. 97%; Fluka),  $\text{Ti}(\text{OPr}^i)_4$  (TPT) (purity 99.999%; Aldrich) and  $\text{Ti}(\text{OBu}^n)_4$  (TBT) (Fluka). Commercially provided surfactants [triblock copolymers  $(\text{PEO})_n(\text{PPO})_m(\text{PEO})_n$ : Pluronic P123 ( $n = 20$ ,  $m = 70$ ), Pluronic F127 ( $n = 100$ ,  $m = 70$ ), Pluronic P3100 ( $n < 2$ ,  $m = 17$ ), L35 ( $n = 10$ ,  $m = 17$ ), Synperonic 42 ( $n = 5$ ,  $m = 20$ ), Brij 56 ( $\text{C}_{16}\text{H}_{34}(\text{PEO})_{10}\text{OH}$ )] were dried prior to use by heating at 70 °C under vacuum.<sup>77</sup> Distilled water, ethanol (EtOH absolute, Eurolab Merck Prolabo), isopropyl alcohol ( $^i\text{PrOH}$  purity >99.7%; Carlo Erba), 1-butanol (BuOH, purity >99.5%; Merck), acetylacetone (purity >97%; Fluka), 1,3-propanediol (Aldrich), acetic acid (glacial), freshly distilled tetrahydrofuran (THF) and hydrochloric acid 35% w/v in water (Eurolab Merck Prolabo) were also used to prepare the starting sols. Toluene and  $\text{C}_6\text{D}_6$  (grade NMR) were used as solvents.

### Reactivity of Ti–O building blocks

The clusters  $\text{Ti}_{12}\text{O}_{16}(\text{OPr}^i)_{16}$  (Ti12),  $\text{Ti}_{16}\text{O}_{16}(\text{OEt})_{32}$  (Ti16) and  $\text{Ti}_{18}\text{O}_{22}(\text{OBu}^n)_{26}(\text{acac})_2$  (Ti18) were prepared as previously described, using 10%  $^{17}\text{O}$  enriched water.<sup>53</sup>  $\text{Ti}_{12}\text{O}_{16}(\text{OPr}^i)_{16}$  white powder;  $^{17}\text{O}$  NMR (toluene– $\text{C}_6\text{D}_6$  50 : 50 v/v)  $\delta$  817 ( $\mu\text{-O}$ ), 564 ( $\mu_3\text{-O}$ ), 538 ( $\mu_3\text{-O}$ ), 522 ( $\mu_3\text{-O}$ ) and 517 ( $\mu_3\text{-O}$ );  $^{13}\text{C}$  NMR (toluene– $\text{C}_6\text{D}_6$  50 : 50 v/v)  $\delta$  25.5, 25.6, 26.1, 26.4, 26.7 ( $\text{OCH}(\text{CH}_3)_2$ ), 76.8, 77.6, 80.0, 80.4, 80.6 [ $\text{OCH}(\text{CH}_3)_2$ ].  $\text{Ti}_{16}\text{O}_{16}(\text{OEt})_{32}$ : white crystals;  $^{17}\text{O}$  NMR (toluene– $\text{C}_6\text{D}_6$  50 : 50 v/v)  $\delta$  750 ( $\mu\text{-O}$ ); 563 ( $\mu_3\text{-O}$ ), 555 ( $\mu_3\text{-O}$ ) and 383 ( $\mu_4\text{-O}$ );  $^{13}\text{C}$  NMR (toluene– $\text{C}_6\text{D}_6$  50 : 50 v/v)  $\delta$  20.2, 20.1, 19.9, 19.4, 19.2, 18.8 ( $\text{OCH}_2\text{CH}_3$ ), 73.7, 73.3, 72.4, 72.2, 71.6, 71.2, 70.0, 69.4 ( $\text{OCH}_2\text{CH}_3$ ).  $\text{Ti}_{18}\text{O}_{22}(\text{OBu}^n)_{26}(\text{acac})_2$ : yellow crystals;  $^{17}\text{O}$  NMR ( $\text{C}_6\text{D}_6$ )  $\delta$  757 ( $\mu\text{-O}$ ), 753 ( $\mu\text{-O}$ ), 738 ( $\mu\text{-O}$ ), 545 ( $\mu_3\text{-O}$ ); 508 ( $\mu_3\text{-O}$ ), 340 ( $\mu_4\text{-O}$ ) and 247 ( $\mu_5\text{-O}$ );  $^{13}\text{C}$  NMR (toluene– $\text{C}_6\text{D}_6$  50 : 50 v/v)  $\delta$  26.4 ( $\text{CH}_3$  of acac;  $\text{OCH}_2\text{CH}_2\text{CH}_2\text{CH}_3$ ); 62.4 ( $\text{OCH}_2\text{CH}_2\text{CH}_2\text{CH}_3$ ;  $\text{OCH}_2\text{CH}_2\text{CH}_2\text{CH}_3$ ); 79.8, 78.8, 78.1, 76.6, 76.0, 75.6, 74.7 ( $\text{TiOCH}_2\text{CH}_2\text{CH}_2\text{CH}_3$ ); 128.4 ( $\text{C}_6\text{D}_6$ ); 189.8 ( $\text{CO acac}$ ) and 104 ( $\text{CH acac}$ ).

Crystals isolated from synthesis solutions were dissolved in toluene– $\text{C}_6\text{D}_6$  (50 : 50 v/v) solutions (final concentration ca.  $10^{-2}$  mol  $\text{dm}^{-3}$ ) containing various ratios of nucleophilic species.  $^{13}\text{C}$  and  $^{17}\text{O}$  NMR spectra were recorded with a Bruker AC300 spectrometer, solid state  $^{17}\text{O}$  MAS NMR spectra on a Bruker DSX 400 spectrometer.

### Synthesis of mesostructured titania

**Alkoxide precursors.** A typical synthesis of mesostructured titania hybrid materials in the presence of surfactants was as follows. The surfactant was dissolved in an alcohol; total dissolution of the surfactant might require some minutes heating at 50 °C. Acid and water, if necessary, were added. The  $\text{Ti}(\text{OR})_4$  precursor was added drop by drop under continuous stirring, until dissolution of the freshly formed gel, if necessary. In all cases, the metal-to-surfactant ratios ( $s$ ) were kept between 20 and 150 : 1 the hydrolysis ratio ( $h$ ) was set between 0.056 and 25 : 1 and the HCl : Ti ratio ( $p$ ) varied between 0.015 and 3 : 1. After stirring for prefixed times, two different kinds of products were obtained, depending on the procedures followed: (1) xerogels were obtained upon solvent evaporation when the mixtures were poured in Petri dishes and held at

room temperature or 50 °C; (2) when the reaction mixtures were held under vigorous stirring, a precipitate appeared which was separated by centrifugation at  $10^4$  rpm during 20 min.

**Ti16 as NBB.** Ti16 clusters being sensitive towards water, all handling was in a glove box under argon (water <10 ppm). Hybrids were formed by mixing Ti16 and the amphiphilic polymers in dry THF ( $10^{-2}$  mol  $\text{dm}^{-3}$ );  $s$  was kept between 8 and 50 : 1. Upon mixing under these “dry” conditions there was an appreciable colour change: the initial pale yellow solutions turned to intense yellow or orange. Dark yellow to orange glass-like solids were obtained upon solvent evaporation by placing the solutions in Petri dishes at ambient temperature.

### Characterisation

The as-synthesized solids were analysed by high-angle powder X-ray diffraction using a Philips PW 1830 Generator (copper anode,  $\lambda = 1.5406$  Å). For small-angle measurements the X-ray generator was a rotating copper anode equipped with a small point focus and operated at 50 kV and 30 mA. The set-up is a small-angle diffraction line with variable sample to film distance. Air scattering is reduced by a vacuum pipe. Diffraction patterns are recorded onto photostimulable imaging plates. A vacuum pipe is placed in-between to reduce diffusion by air. A parallel beam is obtained by a combination of a parabolic multilayer monochromator and a bent mirror at right angles. The samples were also observed under transmission electron microscopy (TEM) in a JEOL 100 CX II apparatus at 100–120 kV voltage. For these analyses, microtomed slides of samples embedded in a polymer resin were used. FTIR characterisation was performed in KBr disks.

### Acknowledgements

The authors thank M. Lavergne for the TEM images. Financial support from CNRS and Rhodia (France), CONICET and Fundación Antorchas (Argentine Republic) is gratefully acknowledged. E.S. and G.J.A.A.S.I. are members of Gabbo's FR.

### References and notes

- 1 *Better Ceramics Through Chemistry VII: Organic/Inorganic Hybrid Materials*, ed. B. K. Coltrain, C. Sanchez, D. W. Schaefer and G. L. Wilkes, Materials Research Society, Pittsburgh, 1996; *Hybrid Materials*, ed. R. Laine, C. Sanchez, C. J. Brinker and E. Gianellis, Materials Research Society, Pittsburgh, 1998.
- 2 *Sol-Gel Optics I*, ed. J. D. Mackenzie and D. R. Ulrich, vol. 1328, SPIE, Washington, 1990; *Sol-Gel Optics II*, ed. J. D. Mackenzie, vol. 1758, SPIE, Washington, 1992; *Sol-Gel Optics III*, ed. J. D. Mackenzie, vol. 2288, SPIE, Washington, 1994; *Sol-Gel Optics IV*, ed. J. D. Mackenzie, vol. 3136, SPIE, Washington, 1997; *Sol-Gel Optics V*, ed. B. S. Dunn, E. J. A. Pope, H. K. Schmidt and M. Yamane, vol. 3943, SPIE, Washington, 2000; B. Lebeau and C. Sanchez, *Curr. Opin. Solid State Mater. Sci.*, 1999, **4**, 11.
- 3 G. Ozin, *Chem. Commun.*, 2000, 419.
- 4 C. J. Brinker and G. W. Scherrer, *Sol-Gel Science, The Physics and Chemistry of Sol-Gel Processing*, Academic Press, San Diego, CA, 1990; J. Livage, M. Henry and C. Sanchez, *Prog. Solid State Chem.*, 1988, **18**, 259.
- 5 R. Corriu, *Polyhedron*, 1998, **17**, 925; R. Corriu, *Angew. Chem., Int. Ed. Engl.*, 1996, **35**, 1420.
- 6 B. M. Novak, *Adv. Mater.*, 1993, **5**, 422.
- 7 U. Schubert, N. Hüsing and A. Lorenz, *Chem. Mater.*, 1995, **7**, 2010.
- 8 (a) C. Sanchez and F. Ribot, *New J. Chem.*, 1994, **18**, 1007; (b) P. Judenstein and C. Sanchez, *J. Mater. Chem.*, 1996, **6**, 511; (c) *Matériaux Hybrides*, Série Arago 17, Masson, Paris, 1996; (d) C. Sanchez, F. Ribot and B. Lebeau, *J. Mater. Chem.*, 1999, **9**, 35.
- 9 D. A. Loy and K. J. Shea, *Chem. Rev.*, 1995, **95**, 1431.
- 10 Y. Chujo, *Curr. Opin. Solid State Mater. Sci.*, 1996, **1**, 806.

- 11 S. Mann, S. L. Burkett, S. A. Davis, C. E. Fowler, N. H. Mendelson, S. D. Sims, D. Walsh and N. T. Whilton, *Chem. Mater.*, 1997, **9**, 2300.
- 12 Recent reviews on this subject include (a) C. T. Kresge, M. E. Leonowicz, W. J. Roth, J. C. Vartuli and J. S. Beck, *Nature (London)*, 1992, **359**, 710; (b) J. Y. Ying, C. Mehnert and M. S. Wong, *Angew. Chem., Int. Ed.*, 1999, **38**, 57; (c) T. J. Barton, L. M. Bull, W. G. Klemperer, D. A. Loy, B. McEnaney, M. Misono, P. A. Monson, G. Pez, G. W. Scherer, J. C. Vartuli and O. M. Yaghi, *Chem. Mater.*, 1999, **11**, 2633; (d) D. Zhao, P. Yang, Q. Hou, B. F. Chmelka and G. Stucky, *Curr. Opin. Solid State Mater. Sci.*, 1998, **3**, 111; (e) C. G. Göltner and M. Antonietti, *Adv. Mater.*, 1997, **9**, 431.
- 13 F. Ribot and C. Sanchez, *Comments Inorg. Chem.*, 1999, **20**, 327.
- 14 G. Fu, C. A. Fyfe, W. Schwieger and G. T. Kokotailo, *Angew. Chem., Int. Ed. Engl.*, 1995, **34**, 1499.
- 15 D. M. Antonelli, A. Nakahira and J. Y. Ying, *Inorg. Chem.*, 1996, **35**, 3126.
- 16 G. J. A. A. Soler-Illia and C. Sanchez, *New J. Chem.*, 2000, **24**, 493.
- 17 D. Hoebbel, K. Endres, T. Reinert and I. Pitsch, *J. Non-Cryst. Solids*, 1994, **176**, 179; D. Hoebbel, I. Pitsch and D. Heidemann, *Z. Anorg. Allg. Chem.*, 1991, **592**, 207.
- 18 T. S. Haddad and J. D. Lichtenhan, *Macromolecules*, 1996, **29**, 7302.
- 19 J. D. Lichtenhan, *Comments Inorg. Chem.*, 1995, **17**, 115.
- 20 A. Sellinger and R. M. Laine, *Chem. Mater.*, 1996, **8**, 1592.
- 21 C. Zhang, F. Babonneau, C. Bonhomme, R. M. Laine, C. L. Soles, H. A. Hristo and A. F. Yee, *J. Am. Chem. Soc.*, 1998, **120**, 8380; M.-C. Gravel, C. Zhang, M. Dinderman and R. M. Laine, *Appl. Organomet. Chem.*, 1999, **13**, 336.
- 22 P. A. Agaskar, *J. Chem. Soc., Chem. Commun.*, 1992, 1024.
- 23 C. M. Casado, I. Cuadrado, M. Moran, B. Alonso, M. Barranco and J. Losada, *Appl. Organomet. Chem.*, 1999, **13**, 245.
- 24 I. Hasegawa, Y. Nakane and T. Takayama, *Appl. Organomet. Chem.*, 1999, **13**, 272.
- 25 E. G. Shockey, A. G. Bolf, P. F. Jones, J. J. Schwab, K. P. Chaffee, T. S. Haddad and J. D. Lichtenhan, *Appl. Organomet. Chem.*, 1999, **13**, 311.
- 26 M. T. Pope and A. Müller, *Angew. Chem., Int. Ed. Engl.*, 1991, **30**, 34; *Polyoxometalates: From Platonic Solids to Anti-Retroviral Activity*, ed. M. T. Pope and A. Müller, Kluwer, Dordrecht, 1994.
- 27 P. Judeinstein, *Chem. Mater.*, 1992, **4**, 4.
- 28 P. Judeinstein, *J. Sol-Gel Sci. Technol.*, 1994, **2**, 147.
- 29 N. Ammari, G. Hervé and R. Thouvenot, *New J. Chem.*, 1991, **15**, 607.
- 30 A. Mazeaud, N. Ammari, F. Robert and R. Thouvenot, *Angew. Chem., Int. Ed. Engl.*, 1996, **35**, 1961.
- 31 C. R. Mayer, R. Thouvenot and T. Lalot, *Chem. Mater.*, 2000, **12**, 257.
- 32 C. R. Mayer, R. Thouvenot and T. Lalot, *Macromolecules*, 2000, **33**, 4433.
- 33 H. Zeng, G. R. Newkome and C. L. Hill, *Angew. Chem., Int. Ed.*, 2000, **39**, 1772.
- 34 G. Kickelbick and U. Schubert, *J. Chem. Soc., Dalton Trans.*, 1999, 1301.
- 35 U. Schubert, E. Arpac, W. Glaubitt, A. Helmerich and C. Chau, *Chem. Mater.*, 1992, **4**, 291.
- 36 G. Trimmel, P. Fratzl and U. Schubert, *Chem. Mater.*, 2000, **12**, 602.
- 37 C. Sanchez, G. J. A. A. Soler-Illia, L. Rozes, A.-M. Caminade, C.-O. Turrin and J.-P. Majoral, *Mater. Res. Soc. Symp. Proc.*, 2000, **628**, in press; G. J. A. A. Soler-Illia, M. K. Boggiano, L. Rozes, A.-M. Caminade, C.-O. Turrin, J.-P. Majoral and C. Sanchez, *Angew. Chem.*, 2000, in press.
- 38 F. Banse, F. Ribot, P. Tolédano, J. Maquet and C. Sanchez, *Inorg. Chem.*, 1995, **34**, 6371.
- 39 F. Ribot, C. Eychenne-Baron and C. Sanchez, *Phosphorus, Sulfur Silicon Relat. Elem.*, 1999, **150**, 15141.
- 40 F. Ribot, F. Banse, F. Diter and C. Sanchez, *New J. Chem.*, 1995, **19**, 1145.
- 41 F. Ribot, C. Eychenne-Baron and C. Sanchez, in *Hybrid Materials*, ed. R. Laine, C. Sanchez, C. J. Brinker and E. Giannelis, Materials Research Society, Pittsburgh, 1998, p. 29.
- 42 N. Steunou, F. Ribot, K. Boubekeur, J. Maquet and C. Sanchez, *New J. Chem.*, 1999, **24**, 1079.
- 43 V. W. Day, T. A. Eberspacher, W. G. Klemperer and C. W. Park, *J. Am. Chem. Soc.*, 1993, **115**, 8469.
- 44 V. W. Day, T. A. Eberspacher, W. G. Klemperer, C. W. Park and F. S. Rosenberg, *J. Am. Chem. Soc.*, 1991, **113**, 8190.
- 45 V. W. Day, T. A. Eberspacher, Y. Chen, J. Hao and W. G. Klemperer, *Inorg. Chim. Acta*, 1995, **229**, 391.
- 46 R. Schmid, A. Mosset and J. Galy, *J. Chem. Soc., Dalton Trans.*, 1991, 1999.
- 47 N. Steunou, F. Robert, K. Boubekeur, F. Ribot and C. Sanchez, *Inorg. Chim. Acta*, 1998, **279**, 144.
- 48 C. F. Campana, Y. Chen, V. W. Day, W. G. Klemperer and R. A. Sparks, *J. Chem. Soc., Dalton Trans.*, 1996, 691.
- 49 P. Tolédano, M. In and C. Sanchez, *C. R. Acad. Sci., Ser II*, 1991, **313**, 1247.
- 50 Y. W. Chen, W. G. Klemperer and C. W. Park, *Mater. Res. Soc. Symp. Proc.*, 1992, **271**, 57.
- 51 H. E. Katz, M. L. Schilling, S. M. Stein, R. S. Hutton and G. N. Taylor, *Chem. Mater.*, 1995, **6**, 1534.
- 52 K. Nakamoto, *Infrared and Raman Spectra of Inorganic and Coordination Compounds*, Wiley, New York, 4th edn., 1986, p. 220; S. Doeuff, M. Henry, C. Sanchez and J. Livage, *J. Non-Cryst. Solids*, 1987, **89**, 206; S. Doeuff, Y. Dromzee, F. Taulelle and C. Sanchez, *Inorg. Chem.*, 1989, **28**, 4439.
- 53 E. Scolan, C. Magnenet, D. Massiot and C. Sanchez, *J. Mater. Chem.*, 1999, **9**, 2467.
- 54 J. Blanchard, C. Bonhomme, J. Maquet and C. Sanchez, *J. Mater. Chem.*, 1998, **8**, 985.
- 55 M. Åberg and J. Glaser, *Inorg. Chim. Acta*, 1993, **206**, 53; D. T. Richens, L. Helm, P. A. Pittet and A. E. Merbach, *Inorg. Chim. Acta*, 1987, **132**, 85.
- 56 N. Launay, A. M. Caminade, R. Lahana and J. P. Majoral, *Angew. Chem., Int. Ed. Engl.*, 1994, **33**, 1589; C. Galliot, C. Larré, A. M. Caminade and J. P. Majoral, *Science*, 1997, **277**, 1971 and references therein.
- 57 D. M. Antonelli and J. Y. Ying, *Angew. Chem., Int. Ed. Engl.*, 1995, **34**, 2014.
- 58 S. Cabrera, J. El-Haskouri, J. Alamo, A. Beltrán, S. Mendioroz, M. D. Marcos and P. Amorós, *Adv. Mater.*, 1999, **11**, 379.
- 59 T. O. Do, *Langmuir*, 1999, **15**, 8561.
- 60 S. A. Bagshaw, E. Prouzet and T. Pinnavaia, *Science*, 1995, **269**, 1242; E. Prouzet and T. J. Pinnavaia, *Angew. Chem., Int. Ed. Engl.*, 1997, **36**, 516; S. A. Bagshaw and T. J. Pinnavaia, *Angew. Chem., Int. Ed. Engl.*, 1996, **35**, 1102; S. A. Bagshaw, *Chem. Commun.*, 1999, 271.
- 61 G. J. A. A. Soler-Illia and C. Sanchez, private communication.
- 62 Q. Huo, D. I. Margolese, U. Ciesla, D. G. Demuth, P. Feng, T. E. Gier, P. Sieger, A. Firouzi, B. F. Chmelka, F. Schüth and G. Stucky, *Chem. Mater.*, 1994, **6**, 1176.
- 63 P. Alexandridis, D. Zhou and A. Khan, *Langmuir*, 1996, **12**, 2690.
- 64 C. Yu, Y. Yu and D. Zhao, *Chem. Commun.*, 2000, 575.
- 65 M. T. Anderson, J. E. Martin, J. G. Odinek and P. P. Newcomer, *Chem. Mater.*, 1998, **10**, 1490.
- 66 J. Blanchard, F. Ribot, C. Sanchez, P.-V. Bellot and A. Trokiner, *J. Non-Cryst. Solids*, 2000, **265**, 83.
- 67 (a) P. Yang, D. Zhao, D. I. Margolese, B. Chmelka and G. Stucky, *Nature (London)*, 1998, **396**, 512; (b) P. Yang, D. Zhao, D. I. Margolese, B. Chmelka and G. Stucky, *Chem. Mater.*, 1999, **11**, 2813.
- 68 D. Zhao, Q. Huo, J. Feng, B. F. Chmelka and G. D. Stucky, *J. Am. Chem. Soc.*, 1998, **120**, 6024.
- 69 P. Yang, D. Zhao, B. F. Chmelka and G. D. Stucky, *Chem. Mater.*, 1998, **10**, 2033.
- 70 G. Wanka, H. Hoffmann and W. Ulbricht, *Macromolecules*, 1994, **27**, 4145.
- 71 P. Holmqvist, P. Alexandridis and B. Lindman, *Langmuir*, 1997, **13**, 2471.
- 72 B. E. Yoldas, *J. Mater. Sci.*, 1986, **21**, 1086; M. Kallala, C. Sanchez and B. Cabane, *Phys. Rev. E*, 1993, **48**, 3692.
- 73 J. Blanchard, M. In, B. Schaudel and C. Sanchez, *Eur. J. Inorg. Chem.*, 1998, 1115.
- 74 R. H. Yoon, T. Salman and G. Donnay, *J. Colloid Interface Sci.*, 1979, **70**, 483.
- 75 R. Zana, J. Frasc, M. Souillard, B. Lebeau and J. Patarin, *Langmuir*, 1999, **15**, 2603.
- 76 In principle, very similar species are found when using acetylacetone as a condensation inhibitor. However, in the latter case, their surface is likely poisoned by organic acetylacetonate groups, rendering them less hydrophilic.
- 77 Pluronic, Synperonic and Brij are registered trademarks. Some of the texturing agents contain minor quantities of water, as determined by duplicate Karl-Fischer titrations: below 0.3% (F127), ca. 1% (P123 and L35) and 2.5% (Brij 56).